Waste and Biomass Valorization (2022) 13:4911–4923
https://doi.org/10.1007/s12649-022-01827-5

ORIGINAL PAPER

Characterization of Dissolved Organic Matter in Aquatic Macrophytes Derived-Biochars Using Multi-spectroscopic Analyses: Combined Effects of Pyrolysis Temperatures and Sequential Extractions

Bingfa Chen[1] · Kaining Chen[2] · Shiqun Han[1] · Cheng Liu[2] · Muhua Feng[2] · Wei Huang[2] · Hui Cai[3]

Received: 21 February 2022 / Accepted: 21 May 2022 / Published online: 9 June 2022

Abstract

Dissolved organic matter in biochars (BDOM) influences the latter's environmental applications. This study applied multiple spectra methods to expound the characteristics of BDOM in aquatic macrophytes (*Alternanthera philoxeroides*) biochars produced at different pyrolysis temperatures under sequential extractions (room-temperature water, hot water and a weak base). The results showed that the feedstock and the biochar produced at 200 °C, biochars produced at 300–500 °C and above 600 °C were unstable, metastable and stable, respectively, according to the release of dissolved organic carbon. One protein-like and four humic-like fluorophores were identified. The BDOM were dominated by humic-like components, and the pyrolysis of fluorescent components was hysteretic compared to the non-fluorescent materials. In addition, the relative molecular weight, aromaticity, and hydrophobicity of BDOM increased correspondingly under sequential extractions. High pH/temperature of extracting solution will lead to the BDOM with higher humification degree. This study also indicates humic acid and polysaccharide, as the fluorescent substance and the non-fluorescent substance, respectively, were more sensitive to pyrolysis temperature and changed firstly under sequential extractions. This study was beneficial for understanding the characteristics of BDOM at the molecular level and for predicting the possible effects and processes of biochars before large-scale applications.

Graphical Abstract

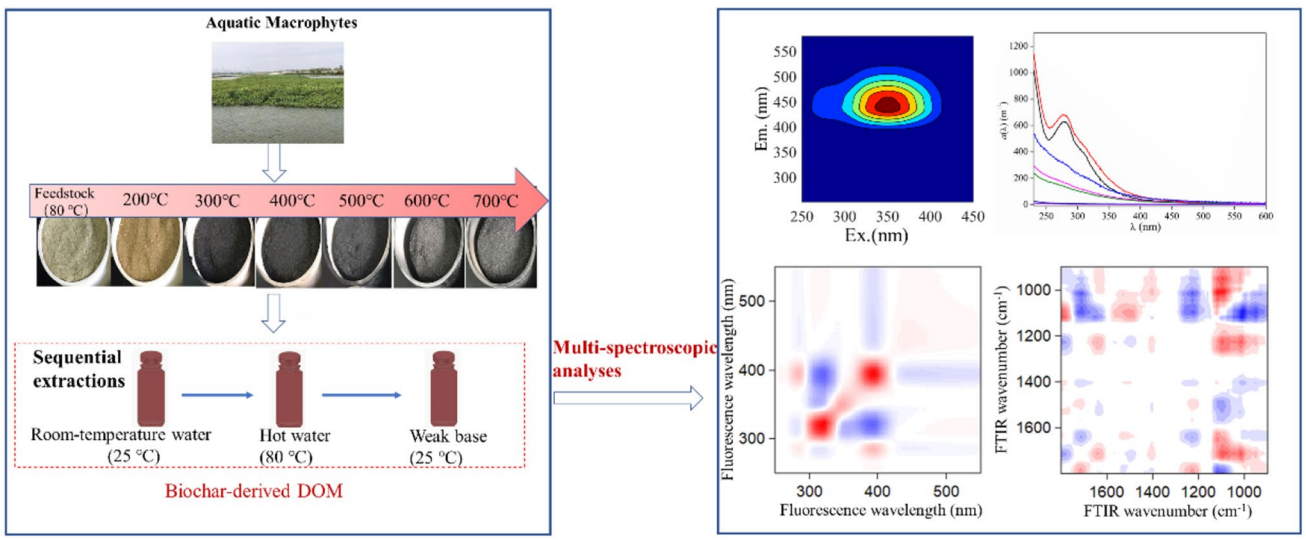

Keywords Biochar · Pyrolysis temperature · Dissolved organic matter · Sequential extractions · Multi-spectroscopic investigations

Extended author information available on the last page of the article

Statement of Novelty

Converting the biomass into biochar is beneficial both win-win in environment and economy. However, potential release of dissolved organic matter derived from biochar (BDOM) influences the latter's environmental applications. BDOM accessed by sequential extraction with different extracting solutions, which include different dissolved organic matter (DOM) fractions, may be a promising strategy to perform research on BDOM, compared to the single water extraction in previous studies. Multi-spectroscopic investigations are promising strategies for obtaining a deep understanding the properties of DOM. Combined effects of pyrolysis temperatures and sequential extractions on the characteristics of BDOM were expounded innovatively using multi-spectroscopic investigations in this study. Our conclusions were beneficial for understanding the characteristics of BDOM at the molecular level and for predicting the possible environmental effects of biochars.

Introduction

Dissolved organic matter (DOM), as an active and complicated mixture of organic components, plays a momentous role in the aquatic environment [1]. Biochars, produced at relatively low temperatures by oxygen-limiting or oxygen-absent pyrolysis of organic material, were applied widely [2–4]. However, biochars are important DOM sources, which containing active components and participating in the biogeochemical processes of materials and the cycles of carbon in the environment [5, 6]. Obviously, quantitative and qualitative studies of biochars derived-DOM (BDOM) are necessary before they can be further used in large-scale applications.

Generally, the release and properties of BDOM will vary with different environmental conditions [7, 8]. Previously, single extraction with the most common extraction solution being deionized water was performed to determine the most labile fractions in BDOM, which were most easily released into the environment [9–11]. However, biochars will experience different conditions in practical applications, for example, biochars can be used in relative high temperature or alkaline environment [12, 13]. After the most labile fractions released into the environment, the remanent components may still have release potential with temperature or pH changed. Therefore, individual extraction method was insufficient to comprehensively determine the properties of BDOM. Sequential extractions with different extracting solutions, which include different fractions with diverse characteristics of DOM, may be a promising strategy to perform research on BDOM [14, 15]. The corresponding characteristics of BDOM are also directly related to the pyrolysis temperatures [9]. However, the release potential and characteristics of BDOM in consideration of pyrolysis temperatures under sequential extractions need to be studied comprehensively.

Some researches have been carried out to determine the characteristics of DOM by a series of methods, e.g., chromatographies, mass spectrometries and multi-spectroscopic analyses [16–18]. Among them, multi-spectroscopic analyses, consisting of ultraviolet visible spectroscopy (UV–Vis), fourier transform infrared spectroscopy (FTIR), excitation emission matrix spectroscopy (EEMs) and synchronous fluorescence spectroscopy (SF) are proven to be promising techniques for their sensitivities, non-destructivities, simplicities, and abundant information obtained [13, 21, 22]. Recently, EEMs–parallel factor analysis (PARAFAC) was applied to provide more insight into the DOM characteristics, such as the fate and source of DOM [19, 20]. Furthermore, two-dimensional correlation spectroscopy (2D-COS) combined with SF and FTIR (2D SF COS and 2D FTIR COS) possess the merits to improve spectral resolutions and selectivities, to deconvolute overlapping peaks and to recognize the response order of spectral changes due to the external disturbances [21, 22]. Therefore, the above multi-spectroscopic investigations are hopeful strategies for acquiring a profound and particular understanding of the BDOM properties.

Aquatic macrophytes are important primary producers in aquatic environments [23]. However, harvesting plant biomass timely is necessary for avoiding reentering nutrients into aquatic environments after the degradation of plant residuals [24, 25].Therefore, in this study, we chose representative aquatic macrophyte, *Alternanthera philoxeroides* (ALP), to produce biochars at different pyrolysis temperatures (200–700 °C). Feedstocks were scythed in wild growing state because of they will block the water surface. In this study, we aim to (1) quantify the release and (2) study the properties of DOM in aquatic macrophytes biochars produced at different pyrolysis temperatures under sequential extractions using UV–Vis, EEM–PARAFAC, 2D SF COS and 2D FTIR COS. This study will provide a promising strategy to understand the characteristics of BDOM comprehensively and to predict the possible effects and processes of biochars before large-scale applications.

Materials and Methods

Production of the Biochars

ALP feedstocks were collected from the littoral zones of Lake Chaohu (Estuary of Shiwuli River in Hefei city) in August 2019. The pretreatment processes of the ALP feedstocks and pyrolysis conditions were described in our previous study [6]. The pyrolysis temperatures were set to 200 °C, 300 °C, 400 °C, 500 °C, 600 °C and 700 °C. Biochars samples are referred to ALPX00, with X00 indicating the pyrolysis temperatures. All biochar samples were ground, and passed through 0.15 mm sieve prior to the extraction experiments.

The yields of biochars were determined based on mass balance as a percentage. The pH was determined with at a mass/volume ratio of 1:10 in deionized water after shaking at 150 rpm for 24 h [26]. Ash content was measured according to standard test method [27]. The C, H, and N contents were measured using an elemental analyzer (Vario Macro cube) and the oxygen content was calculated by weight difference.

DOM Sequential Extractions Experiments

DOM was obtained by a modified sequential extraction method [7, 14]. Briefly, room-temperature deionized water, hot (80 ± 1 °C) deionized water, and then 50 mM NaOH (room temperature) were used to extracting sequentially with individual extracting time of 16 h and a mass/volume ratio of 1.00 g/40 mL. The suspension was centrifuged (4000 rmp for 15 min), and filtered using 0.45 μm microfiber filters (Membrana, Germany). The solid residue was washed with 5 mL of deionized water twice and dried in an oven under 50 °C before the next extraction for mass calibration. Thus, three types of BDOM are hereby denoted as D1 (room- temperature water), D2 (hot water), and D3 (weak base). Triplicate parallel samples were prepared for each step during the sequential extractions. Extraction with room-temperature water was performed to determine the most labile organic carbon. Hot water extraction usually was applied to estimate the labile carbon content of biomaterials that is available for microflora in the short term. A weak base solution was used widely to estimate the relative stabiliity and humic-like substances in biomaterials [14, 15].

Analytical Methods

Dissolved Organic Carbon Analysis

Dissolved organic carbon (DOC) in each extracting solution was determined by a Shimadzu total organic carbon analyzer (TOC-V). The water-soluble DOC contents (mg/g) under sequential extractions were calculated by multiplying the DOC concentration (mg/L) by V/M, where V and M represent the volume of extraction solution (L) and the mass of the biochar (g), respectively.

Spectral Measurements

The UV–vis spectroscopy was obtained with a spectrophotometer (UV-2700, Shimadzu), and the fluorescence spectra were recorded from a fluorescence spectrofluorometer (HORIBA Fluorolog-3). The EEM spectroscopy was recorded CCD detector. Added precaution is needed to ensure the DOM solution were optically dilute (the UV absorbance at 260 nm below 0.1) before fluorescence measurements in order to reduce any inner filter effect [28]. The absorption spectra ranges were 220–800 nm with 1-nm intervals and the average absorbance at 700–800 nm was applied as base line to correct the absorbance spectra. The excitation and emission spectra were recorded between 250 and 450 nm at 5-nm intervals, and between 250 and 580 nm at 1-nm intervals, respectively. The DOC content of all samples was diluted to the same concentration (approximately 7 mg/L, this concentration was necessary to reduce the inner filtering effects with greatest extent [6]) prior to the SF spectra determination except the DOM solutions extracted from ALP600 and ALP700 with weak base due to the DOC content was insufficient for further dilution. SF spectra were also recorded using the same spectrofluorometer but with a PMT detector. Detailed information on fluorescence measurements were expounded in our previous study [6, 19]. After above analyses, the remaining solutions were freeze-dried and dried solid matters were used to FTIR spectroscopy scanning with a FTIR spectrometer (Nicolet iS50). The FTIR spectra ranges were 4000 cm^{-1} to 400 cm^{-1} at 2 cm^{-1} resolution and with 64 scans.

Chemometric Analysis

Absorption coefficients [$a(\lambda)$] of DOM were calculated as the following equation: $a(\lambda) = 2.303 \times A(\lambda)/l$, $A(\lambda)$ is the corrected absorbance at wavelength λ, and l is the cuvette path length in meters. We applied E_2: E_3 [$a(250)$: $a(365)$] to evaluate relative molecular weight (MW) variations (negative correlation) [29]. The value of $SUVA_{254}$ was calculated by $a(254)$/DOC to indicate the relative aromaticity variations of DOM, relative aromaticity increased as the $SUVA_{254}$

increased [30]. In addition, fluorescent Indices include humification index (HIX) and biological index (BIX) obtained from EEMs were used to further characterize the fluorescent dissolved organic matter (FDOM) [31, 32]. The HIX increases with the increasing of humification of FDOM. High BIX (> 1) values indicating higher autochthonous biological activities and freshly FDOM released [31, 33]. The drEEM toolbox [34] was used to perform the modeling process of PARAFAC. Detailed information on PARAFAC modeling was expounded in our previous study [19]. Five components were identified by PARAFAC modeling and the maximal fluorescent intensity (F_{max}) was considered to be proportional to the true concentrations of the different FDOM components. 2Dshige freeware developed by Kwansei-Gakuin University was used to perform 2D-COS analyses of SF and FTIR and the detailed principles was expounded by [35].

Statistical Analysis

Statistical analyses were conducted by Statistical Program for Social Sciences 18.0 software. Significance levels are reported as not significant ($p \geq 0.05$) or significant ($p < 0.05$).

Results and Discussion

Fundamental Properties of Biochars

All the basic physicochemical properties were presented in Supplementary information (S1).

Variations in DOC Quantity

The mean DOC concentrations and percentage DOC distributions under sequential extractions of the biochars are shown in Fig. 1. In general, the variations in the total contents of DOC occurred in three stages: (1) high release of fresh feedstocks and ALP200 with three extracts in which the total contents of DOC exceeded 100 mg/g. (2) relatively low release as the pyrolysis temperature in the range of 300–500 °C. Biochars produced at 300–500 °C still had DOC release potential when the pH or temperatures increased. (3) no obvious release as the pyrolysis temperature higher than 600 °C (Fig. 1a), indicated that labile carbon compounds disappeared, stable carbon remained, and environmental stabilities of biochars were reinforced. These results were also supported by the conclusion of fundamental properties (Table S1), which showed that the stabilities of the biochars enhanced as the pyrolysis temperatures increased. Specifically, the ALP200, which was in a partially pyrolyzed state (Fig. S1), released more total DOC contents than the other biochars ($p < 0.05$) (Fig. 1a), indicating biochar in this state facilitated more DOC releases into the water. The release of DOC of D1 with the pyrolysis temperature below 500 °C were significantly higher than that of D2 and D3 ($p < 0.05$), indicating that ALP and biochars produced at these temperature ranges consist of more labile and active organic carbon, whereas the results were opposite with the pyrolysis temperature at 600–700 °C.

UV–Visible Spectral Absorption

The absorption spectra of BDOM extracted via three extracting solutions are showed in Fig. S2. The BDOM spectral curves decreased exponentially generally near zero absorption at 600 nm as wavelength increased, except obvious peaks appeared at 250–350 nm for the ALP and ALP200 for all three extracting solutions. The absorbance shoulder was ascribed to the abundant chromophores contained aromatic and phenolic components with conjugated C=C and C=O double bonds that have strong absorbance in this range [36]. The disappearance of this absorbance shoulder at ALP300

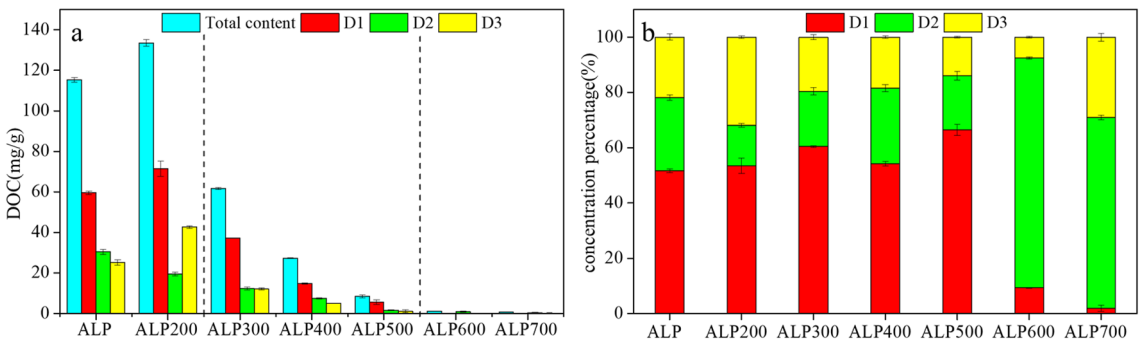

Fig. 1 The contents of DOC (**a**) and percentage distribution of the total DOC contents (**b**) extracted from *Alternanthera philoxeroides* and corresponding biochars (D1 for room-temperature water extraction, D2 for hot water extraction, and D3 for weak base extraction (50 mM NaOH). All values are given as the mean and the standard deviation (error bar) from three replicates (n = 3)

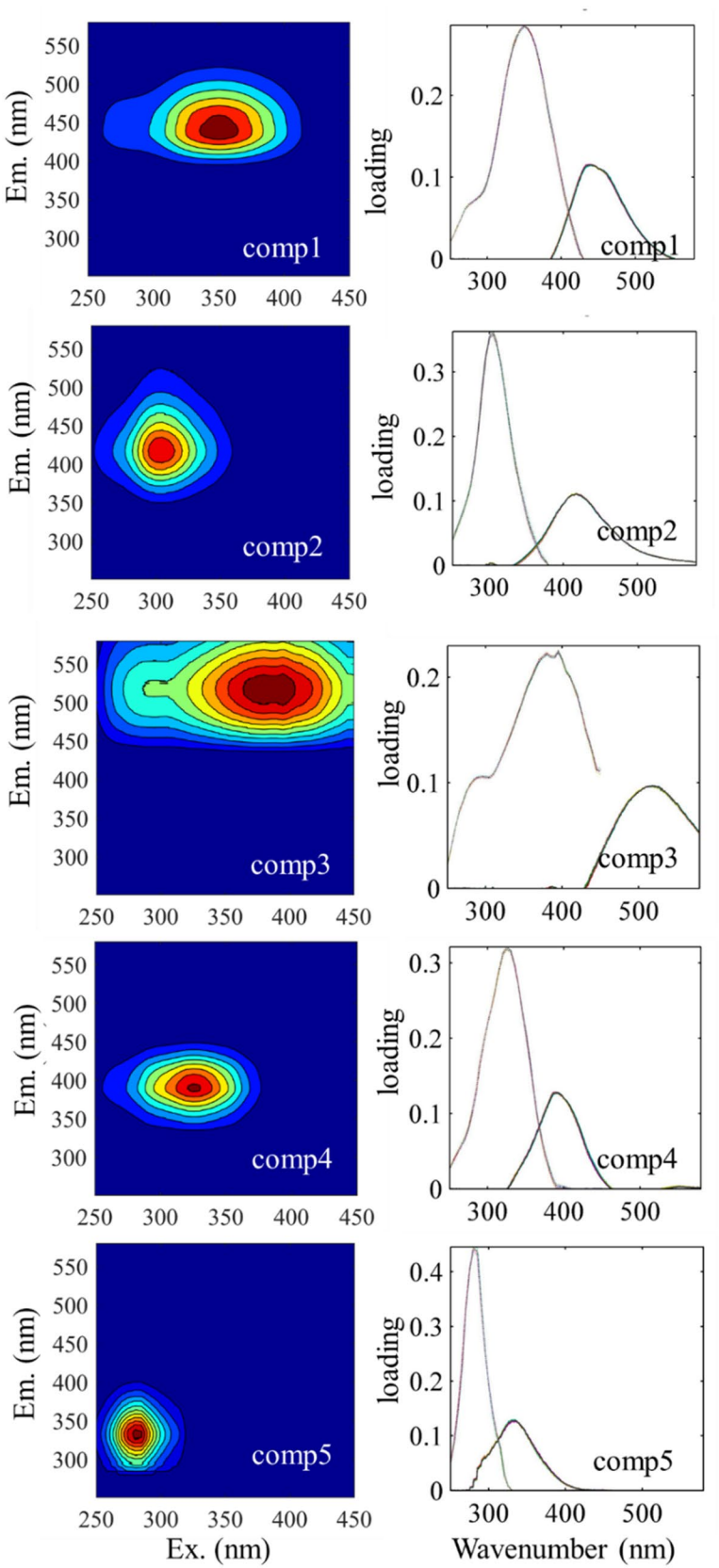

Fig. 2 Five identified components from PARAFAC analysis (left) and loadings from split-half validation results for the corresponding components, including the excitation and emission spectra of six unique split halves and the overall model (right). For each component, these loading lines are nearly superimposed, and the similar shape of the components provides a nearly perfect validation of the fluorescence signatures. Comp1(C1), comp2(C2), comp3(C3) and comp4(C4) were humic-like components, comp5 was protein-like material. Ex. and Em. are the excitation and emissions wavelengths, respectively

showed that these organic compounds have decomposed. As the pyrolysis temperature above 300 °C, these DOM spectral curves were similar to those reported previously for natural organic matter from aquatic or edaphic environments [11, 37], suggesting that using biochars of this study in application would add chromophores to the natural environment. Overall, the absorption coefficients reduced as the pyrolysis temperature increased. In general, the absorption coefficients of ALP200, especially for room-temperature extracts and weak base extracts, were significantly higher than that of biochars produced at the other temperatures ($p < 0.05$), indicating that ALP200 facilitated more chromophores releases into water, which were consistent with the contents of DOC (Figs. 2, S2).

The values of E_2:E_3 and $SUVA_{254}$ were analyzed to further elaborate the biogeochemical characteristics of BDOM. As shown in Table 1, as a whole, the values of E_2:E_3 varied in the order of D1 > D2 > D3 with the pyrolysis temperature under 500 °C, which indicated that relative MW increased with the extraction sequentially. This also means that the labile BDOM had a relatively low MW compared to stable and humified BDOM, this result was similar to previous study, in which the relative MW was higher in base extraction [38]. Overall, the mean values of E_2:E_3 of D1 and D2 increased when the pyrolysis temperature being raised, indicates that an elevated pyrolysis temperature will result in a decrease of the relative MW of D1 and D2 (Table 1). This result was similar to [39] which showed that water-extractable BDOM with a higher pyrolysis temperature was dominated by low MW acids and neutrals.

$SUVA_{254}$ is a reasonable parameter used to evaluate the aromaticity of DOM in which the DOM with lower value of $SUVA_{254}$ has a lower aromaticity and hydrophobicity [30, 40]. Generally, a high SUVA value of > 4 L mg^{-1} m^{-1} refers to the compounds with high hydrophobicity and aromaticity, while a low $SUVA_{254}$ of < 3 L mg^{-1} m^{-1} indicates mainly a hydrophilic material [41]. In this study, the values of $SUVA_{254}$ of D1 were lower than or close to 3 L mg^{-1} m^{-1}, whereas the values of $SUVA_{254}$ values increased with the further sequential extraction, and the $SUVA_{254}$ exceeded 4 L mg^{-1} m^{-1} when the pyrolysis temperature at 300–500 °C of D2 and D3 (Table 1). This indicated that the aromaticity and hydrophobicity of D2 and D3 was enhanced, and single deionized water extraction only obtained hydrophilic and low aromatic DOM. In addition, the $SUVA_{254}$ of D2 and D3 increased as the pyrolysis temperature increased to 500 °C and then reduced at 600 °C and 700 °C (Table 1). Labile compounds (cellulose, hemicellulose, etc.) are degraded preferentially at a pyrolysis temperature lower than 500 °C [42], which resulted in producing more aromatic structures. However, aromatic matter is continually decomposed when the pyrolysis temperature is above 500 °C [14], which may account for the variation in $SUVA_{254}$. The aromaticity and hydrophobicity variations of BDOM under 500 °C were also supported by the characteristics of the elemental and functional groups analysis (Table S1), which showed that hydrophobicity, aromaticity enhanced as the pyrolysis temperature increased. High hydrophilcity and low aromaticity of the BDOM of D1, which means abundant oxygen-containing groups as active sites preferentially participating in the complexation of metals. Thus, this influences the heavy metal speciation and migration when biochars are applied for remediation of metal-polluted soils or sediments need be focused.

Characteristics and Abundances of EEM–PARAFAC Components

We uploaded PARAFAC models to OpenFluor database (http://www.openfluor.org) to compare with the published data, the excitation and emission similarity score was set as 0.95 [43] (Fig. 2; Table S2). C1 component (Ex/Em = 350 nm/440 nm) is associated with a group of high relative aromaticity and MW, similar to the components of lignin and tannin [44–46]. C2 component had an excitation

Table 1 Measured E_2:E_3 and $SUVA_{254}$ (L mg^{-1} m^{-1}) of DOM extracted from D1 (room-temperature water extraction), D2 (hot water extraction) and D3 (weak base extraction)

	D1		D2		D3	
	E_2:E_3	$SUVA_{254}$	E_2:E_3	$SUVA_{254}$	E_2:E_3	$SUVA_{254}$
ALP	3.93 ± 0.03e	1.72 ± 0.03c	4.00 ± 0.24c	1.71 ± 0.06 cd	2.47 ± 0.08b	2.14 ± 0.00b
ALP200	4.82 ± 0.05e	3.00 ± 0.07a	3.33 ± 0.08c	2.63 ± 0.06c	2.33 ± 0.01b	3.74 ± 0.08ba
ALP300	5.36 ± 0.06e	2.77 ± 0.04b	4.41 ± 0.05c	4.19 ± 0.38b	3.01 ± 0.04b	4.77 ± 0.18ba
ALP400	6.18 ± 0.19e	1.88 ± 0.01c	6.20 ± 0.34bc	4.14 ± 0.10bc	4.80 ± 1.07a	4.85 ± 0.12b
ALP500	9.76 ± 1.57b	0.68 ± 0.14d	7.34 ± 0.15b	4.83 ± 0.89a	ND	4.98 ± 0.64a
ALP600	9.38 ± 0.93c	ND	9.27 ± 0.51ab	2.51 ± 0.83cd	ND	2.92 ± 1.12ba
ALP700	22.68 ± 3.35a	ND	10.76 ± 3.24a	0.94 ± 0.04d	ND	2.74 ± 0.13ba

Different letters for each column indicate significant differences among different pyrolysis temperatures ($p < 0.05$)

ND not detected

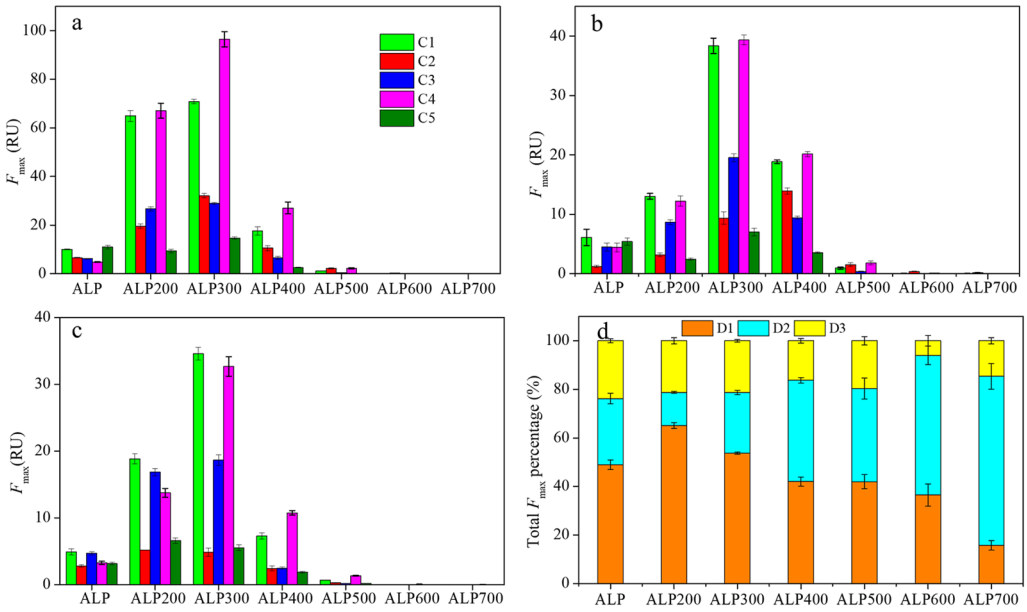

Fig. 3 The maximal fluorescent intensities (F_{max}) of identified fluorescent components (**a** room-temperature water extraction, **b** hot water extraction, **c** weak base extraction) and percentage distribution of FDOM under sequential extractions (**d**). All values are given as the mean and the standard deviation (error bar) from three replicates (n = 3). The F_{max} were shown in Raman units (RU)

maximum at 305-nm and emission maximum at 417-nm, and is thought to correspond to low MW and aliphatic molecules of the humic-like component [47–49]. Two excitation wavelengths at 295 nm and 395 nm and an emission wavelength at 518 nm were found in C3 component, which representing an unidentified humic-like component and only being previously reported by [19] and [50]. C4 component with the peak at the Ex/Em of 325/389 nm is similar to a UV-A humic-like, low MW component and similar to the semiquinone fluorophore [50–52]. C5 component with the peak at the Ex/Em of 280/334 nm was associated with protein-like component that is susceptible to being degraded by microorganisms [53, 54].

To better expound the characteristics of FDOM released from the biochars, the F_{max} of the individual fluorescent component and the F_{max} percentage variations were evaluated (Fig. 3). Specially, the peak values of F_{max} were found at 300 °C, which was backward compared to the DOC release peak at 200 °C, indicating fluorescent components still be retained as the non-fluorescent materials were pyrolyzed. As the pyrolysis temperature got to 600 °C, the F_{max} of all three DOM solutions were negligible. In addition, humic-like materials were significantly higher than protein-like component ($p < 0.05$), indicating that biochars may be non-negligible humic-like substances sources of natural environments when being taking into engineering applications [55].

In this study, the D2 had the highest HIX values among the three BDOM soultions ($p < 0.05$) (Table 2), this result indicating that the high temperature of extracting solution will lead to the DOM with higher humification degree, [56]

Table 2 Measured humification index (HIX) and biological index (BIX) of DOM extracted from D1 (room-temperature water extracts), D2 (hot water extracts) and D3 (weak base extracts)

	D1		D2		D3	
	HIX	BIX	HIX	BIX	HIX	BIX
ALP	1.21 ± 0.03d	0.51 ± 0.01e	1.40 ± 0.11e	0.83 ± 0.07c	3.09 ± 0.20d	0.82 ± 0.04b
ALP200	4.34 ± 0.07c	0.94 ± 0.01b	5.73 ± 0.22c	1.04 ± 0.01a	5.09 ± 0.14c	0.82 ± 0.04b
ALP300	4.44 ± 0.03c	1.03 ± 0.00a	5.78 ± 0.13c	0.93 ± 0.01b	5.14 ± 0.12b	1.04 ± 0.04ab
ALP400	6.11 ± 0.30b	0.92 ± 0.01b	7.48 ± 0.03b	0.77 ± 0.00d	5.89 ± 0.19a	1.21 ± 0.06a
ALP500	9.03 ± 0.83a	0.68 ± 0.01c	10.86 ± 0.65a	0.70 ± 0.00e	6.32 ± 0.08a	1.13 ± 0.02ab
ALP600	8.59 ± 0.41a	0.57 ± 0.00d	5.38 ± 0.12c	0.62 ± 0.02f	2.40 ± 0.83e	0.81 ± 0.07b
ALP700	3.50 ± 1.11c	0.52 ± 0.03e	3.47 ± 0.23d	0.53 ± 0.00g	1.97 ± 0.43e	0.61 ± 0.08b

Different letters for each column indicate significantly different ($p < 0.05$, one-way ANOVA) among different biomaterials

also reported that the extracting temperature significantly influences the humification degree of DOM. In addition, the BIX values of all DOM solutions were 0.52–1.32, and almost were less than 1, indicating that the DOM solutions had weaker biological activities. Specifically, BIX decreased as the pyrolysis temperature increased for D1 and D2 ($p < 0.05$), indicating BDOM derived from biochars produced at higher temperatures had lower fresh DOM and weaker biological activities.

For three BDOM extractions, ALP feedstock had lowest HIX, then the HIX increased as the pyrolysis temperature rose up to 500 °C, meaning that the humification enhanced as the pyrolysis temperature increased. However, the HIX values then sharply reduced (Table 2), which may be attributed to the polymerized DOM under 500 °C further being decomposed and rearranged as the pyrolysis temperature above 600 °C [57]. [11] found that the degree of BDOM humification was the dominant factor in its binding capacity of polycyclic aromatic hydrocarbon. Biochar amendment will enhance the humification of soils [58]. Therefore, optical analysis and full consideration of the changes in the BDOM characteristics are indispensable for minimizing toxic organic compounds in soil or sediment environment.

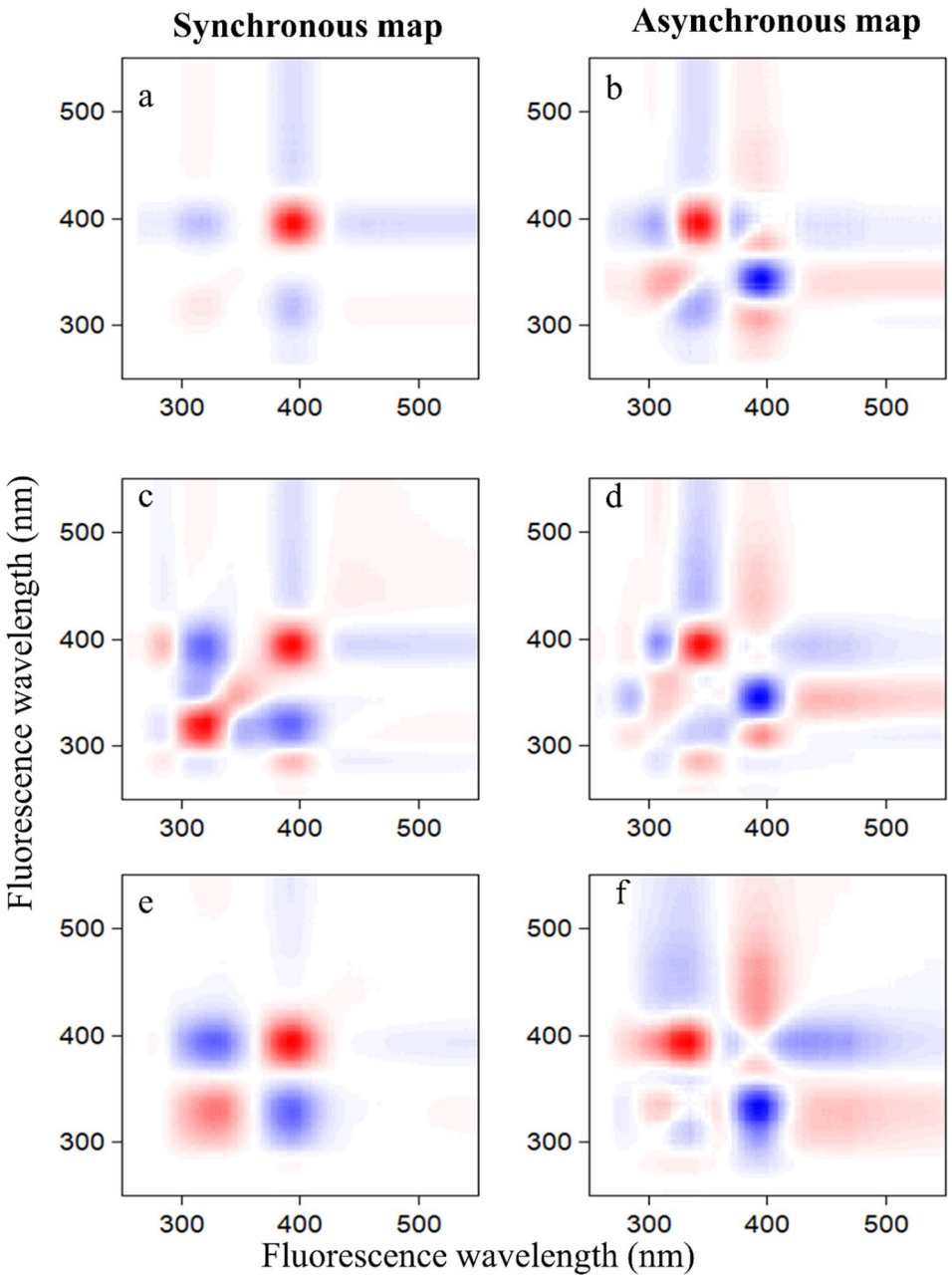

Fig. 4 Two-dimensional correlation analysis of synchronous fluorescence spectra of biochar derived-DOM with sequential extractions (**a** and **b,** room-temperature water extracts; **c** and **d,** hot water extracts; **e** and **f,** weak base extracts)

2D-COS Combined with SF Spectra

The changes of the SF for BDOM under sequential extractions were shown in Fig. S3. Specifically, obvious humic-like peaks appeared in the 300–450 nm band, which including fulvic acid and humic acid with peaks at 300–380 nm, 380–450 nm, respectively [59]. The fluorescence intensities of the peak increased as the pyrolysis temperatures increased to 300 °C or 400 °C then decreased as the pyrolysis temperatures decreased, which were consistent with the results of EEMs-PARAFAC.

2D SF COS were acquired to providing the sequential change order of fluorescent components of BDOM (Fig. 4). Two main peaks along the diagonal of the synchronous spectra were 316 nm (fulvic acid) and 394 nm (humic acid) for D1 solution, 328 nm (fulvic acid) and 392 nm (humic acid) for D3 solution, respectively. However, five main autocorrelation peaks were found in in the synchronous spectra of D2 solution, including 284 nm (protein-like substances), 320 nm (fulvic acid), 344 nm (fulvic acid), 394 nm (humic acid) and 440 nm (humic acid), indicating fluorescent components were more sensitive to hot water extracts. One negative cross-peaks at 316/394 nm and 328/392 nm for D1 and D3 solution, respecitvely, and four negative cross-peaks at 284/320 nm, 284/440 nm, 320/394 nm and 394/440 nm for D2 solution, whereas only one positive crosspeak at 284/394 nm for D2 solution (Table S3), indicating that almost all fluorophore signals did not simultaneously change with each other.

The asynchronous maps showed that the crosspeaks at 316/394 nm for D1 solution, at 320/394 nm for D2 solution and at 328/392 nm for D3 solution were negative, and the crosspeaks at 284/320 nm, 284/394 nm, 284/440 nm, 320/344 nm and 394/440 nm for D2 solution were positive (Table S3). Therefore, the change sequences of fluorophores followed the order humic acid (394 nm) → fulvic acid (316 nm) for D1 solution, humic acid (394 nm) → protein-like substances (284 nm) → fulvic acid (320 nm) → fulvic acid (344 nm) for D2 solution, and humic acid (392 nm) → fulvic acid (328 nm) for D3 solution on the basis of sequential order rule [35]. Obviously, humic acid in biochars was more sensitive and changed firstly in this study, which were inconsistent with results reported by [60], these opposite results were mainly on account of the differences of the feedstock sources.

2D-COS Maps Combined with FTIR Spectra

In order to further investigate the changes of non-fluorescent substances in BDOM. The changes of the FTIR for BDOM under sequential extractions were shown in Fig. S4, obviously, main shoulders changes were showed in the 1800–900 cm^{-1} area, overlapping peaks may hidden the much structural changes in these bands [21]. Therefore, 2D FTIR COS analysis were conducted in this study to explain the BDOM functional groups variations under sequential extractions. As shown in Fig. 5, the autopeaks exhibited in synchronous maps of three BDOM solutions existed obvious differences, six autopeaks at 1709, 1648, 1230, 1097, 1015 and 953 cm^{-1} were exhibited for D1 solution, four autopeaks at 1573, 1492, 1012 and 950 cm^{-1} for D2 solution and four autopeaks at 1610, 1533, 1038 and 945 cm^{-1} for D3 solution. The numbers of autopeaks of D1 were higher than that of D2 and D3, indicating more active functional groups in biochars were sensitive to room-temperature water extracts. The band at 1709 cm^{-1} was assigned to C=O symmetrical stretching vibration of carboxyl [61, 62]. The band at 1648 cm^{-1} correspond to the C=C stretching vibration or C=O stretching vibration in a carboxylic acid [63], the band at 1530 and 1573 cm^{-1} were attributed to C–N, C=N vibration in amide II [61]. The band at 1492 cm^{-1} and 1230 cm^{-1} were associated with benzene ring C=C and phenolic C–O stretching, respectively [64, 65]. The bands at 1097, 1038, 1015, 1012, 953, 950 and 945 cm^{-1} represented C–O stretching of polysaccharide [61, 66].

For synchronous maps, both positive and negative crosspeaks were found from three BDOM solutions (Fig. 5a, c, e), implying that almost all FTIR functional groups signals did not simultaneously change with each other with the increase of pyrolysis temperatures. For asynchronous maps, both positive and negative crosspeaks were also observed (Fig. 5b, d, f), On the basis of the Noda's rule and the peak's signs (Tables S4, S5, S6) [35], the sequential order of FTIR functional groups was polysaccharide C–O at 1097 cm^{-1} → C=C of benzene ring or C=O of carboxylic compound → polysaccharide C–O at 1015 cm^{-1} → polysaccharide C–O at 953 cm^{-1} → C–O of phenolic compound ≈C=O of carboxyl for D1 solution, polysaccharide C–O at 950 cm^{-1} → C–N, C=N of amide II → polysaccharide C–O at 1012 cm^{-1} or polysaccharide C–O at 950 cm^{-1} → benzene ring C=C for D2 solution, and polysaccharide C–O at 945 cm^{-1} → polysaccharide C–O at 1038 cm^{-1} → C=C of the lignin molecules → C–N, C=N of amide II for D3 solution, respectively. Obviously, polysaccharide in three BDOM solution changed firstly, this result was consistent with [60]. In fact, polysaccharide was an active ligand in biochars participated in pollutant migrations [6, 67]. Amide II was the active site of protein-like substances and was not the peak of synchronous map of D1, indicating that protein-like substances were comparatively low in biochars in this study, which was in accord with the conclusions of EEM–PARAFAC and 2D SF COS.

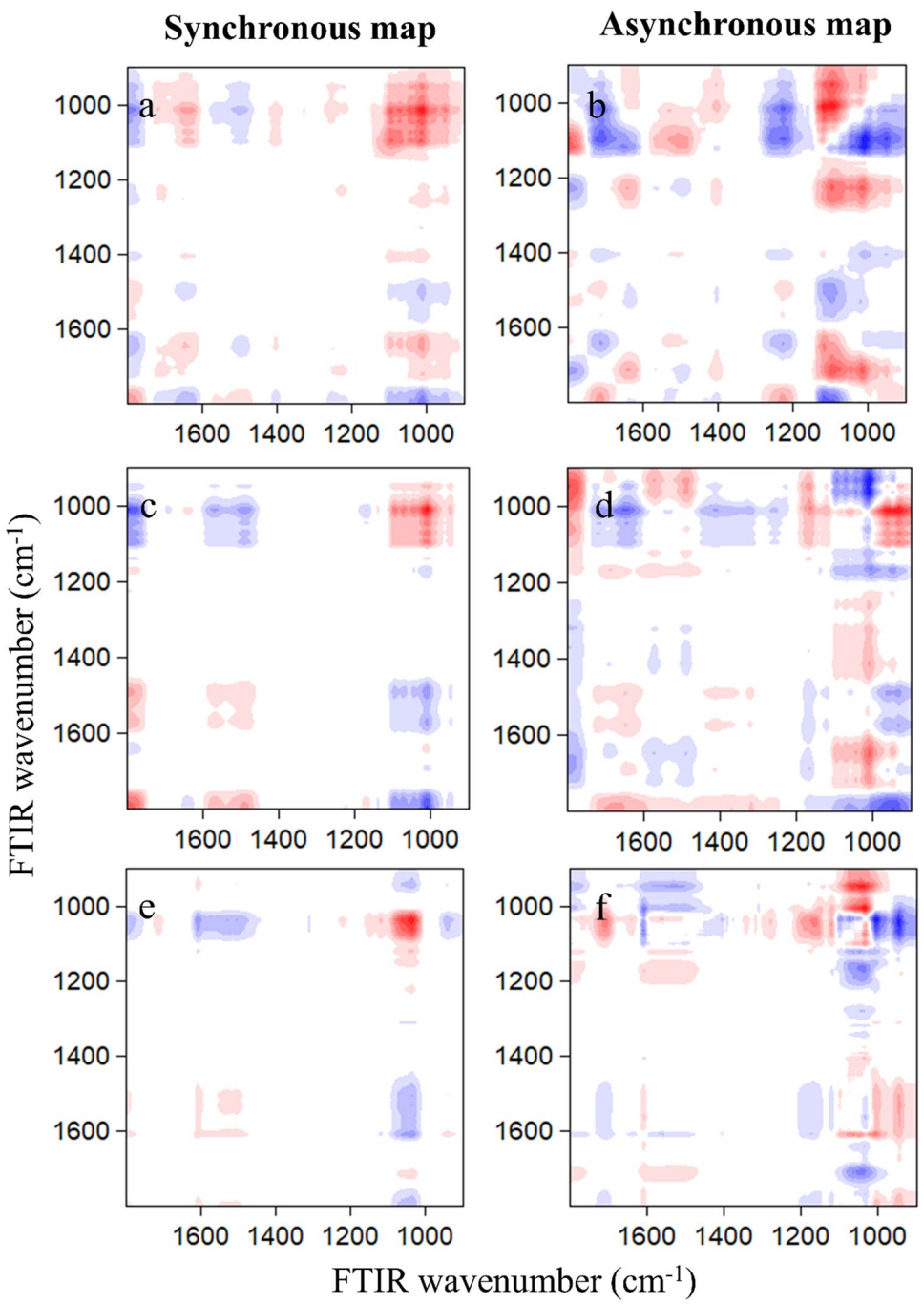

Fig. 5 Two-dimensional correlation analysis of FTIR (1800–900 cm^{-1}) of BDOM with sequential extractions (**a** and **b** room-temperature water extracts; **c** and **d** hot water extracts; **e** and **f** weak base extracts)

Conclusion

UV–Vis, EEM-PARAFAC, 2D SF COS and 2D FTIR COS were applied as promising methods to expound the characteristics of three BDOM solutions with the variates of pyrolysis temperatures. Overall, fresh aquatic macrophytes and biochars produced at 200 °C caused a higher release of BDOM. Biochars produced at 300–500 °C and above 600 °C were metastable and stable, respectively. BDOM in the three extracts was dominated by humic-like components. In addition, the relative MW, aromaticity, and hydrophobicity increased correspondingly under sequential extractions. Pyrolysis of fluorescent components was hysteretic and the corresponding contents reached a peak at 300 °C. An elevated pyrolysis temperature will result in an increase of the relative MW of three BDOM solutions. What's more, the high pH/temperature of extracting solution will lead to the BDOM with higher humification degree. This study also indicates humic acid and polysaccharide, as the fluorescent substance and the non-fluorescent substance, respectively,

were more sensitive and to pyrolysis temperature and changed firstly. Therefore, multi-spectroscopic techniques were promising approaches to understand BDOM thoroughly at the molecular level and to predict the possible effects and processes of aquatic macrophytes biochars before large-scale applications.

Supplementary Information The online version contains supplementary material available at https://doi.org/10.1007/s12649-022-01827-5.

Acknowledgements This research was funded by the National Natural Science Foundation of China (41877544, 41877482, 42077310) and the Major Project for Water Pollution Control of Lake Taihu (No. TH2019201). We thank Yan Yan for his assistances in the DOM sequential extraction experiments.

Data Availability Enquiries about data availability should be directed to the authors.

Declarations

Conflict of interest The authors declare that they have no known competing financial interests or personal relationships that could have appeared to influence the work reported in this paper.

References

1. Sankar, M.S., Dash, P., Singh, S., Lu, Y.H., Mercer, A., Chen, S.: Effect of photo-biodegradation and biodegradation on the biogeochemical cycling of dissolved organic matter across diverse surface water bodies. J. Environ. Sci. **77**, 130–147 (2009)
2. Orooji, Y., Han, N., Nezafat, Z., Shafiei, N., Shen, Z., Nasrollahzadeh, M., Karimi-Maleh, H., Luque, R., Bokhari, A., Klemeš, J.J.: Valorisation of nuts biowaste: prospects in sustainable bio(nano) catalysts and environmental applications. J. Clean. Prod. **347**, 131220 (2022)
3. Gao, Y., Wu, P., Jeyakumar, P., Bolan, N., Wang, H., Gao, B., Wang, S., Wang, B.: Biochar as a potential strategy for remediation of contaminated mining soils: mechanisms, applications, and future perspectives. J. Environ. Manage. **313**, 114973 (2022)
4. Amalina, F., Razak, A.S.A., Krishnan, S., Zularisam, A.W., Nasrullah, M.A.: Comprehensive assessment of the method for producing biochar, its characterization, stability, and potential applications in regenerative economic sustainability—a review. Clean. Mater. **3**, 100045 (2022)
5. Deenik, J.L., Mcclellan, T., Uehara, G., Antal, M.J., Campbell, S.: Charcoal volatile matter content influences plant growth and soil nitrogen transformations. Soil Sci. Soc. Am. J. **74**, 1259–1270 (2010)
6. Chen, B., Zhao, M., Liu, C., Feng, M., Ma, S., Liu, R., Chen, K.: Comparison of copper binding properties of DOM derived from fresh and pyrolyzed biomaterials: insights from multi-spectroscopic investigation. Sci. Total Environ. **721**, 137827 (2020)
7. Uchimiya, M., Hiradate, S., Antal, M.J.: Influence of carbonization methods on the aromaticity of pyrogenic dissolved organic carbon. Energy Fuels **29**, 2503–2513 (2015)
8. Liu, P., Ptacek, C.J., Blowes, D.W., Berti, W.R., Landis, R.C.: Aqueous leaching of organic acids and dissolved organic carbon from various biochars prepared at different temperatures. J. Environ. Qual. **44**(2), 684–695 (2015)
9. Jamieson, T., Sager, E., Guéguen, C.: Characterization of biochar-derived dissolved organic matter using UV–visible absorption and excitation–emission fluorescence spectroscopies. Chemosphere **103**, 197–204 (2014)
10. Smith, C.R., Sleighter, R.L., Hatcher, P.G., Lee, J.W.: Molecular characterization of inhibiting biochar water-extractable substances using electrospray ionization Fourier transform ion cyclotron resonance mass spectrometry. Environ. Sci. Technol. **47**, 13294–13302 (2013)
11. Tang, J., Li, X., Luo, Y., Li, G., Khan, S.: Spectroscopic characterization of dissolved organic matter derived from different biochars and their polycylic aromatic hydrocarbons (PAHS) binding affinity. Chemosphere **152**, 399–406 (2016)
12. Li, Q., Xu, M., Wang, G., Chen, R., Qiao, W., Wang, X.: Biochar assisted thermophilic co-digestion of food waste and waste activated sludge under high feedstock to seed sludge ratio in batch experiment. Bioresour. Technol. **249**, 1009–1016 (2018)
13. You, H., Zhang, Y., Li, W., Li, Y., Feng, X.: Removal of NO_3^-–N in alkaline rare earth industry effluent using modified coconut shell biochar. Water Sci. Technol. **80**, 784 (2019)
14. Wei, S., Zhu, M., Fan, X., Song, J., Peng, P.A., Li, K., Jia, W., Song, H.: Influence of pyrolysis temperature and feedstock on carbon fractions of biochar produced from pyrolysis of rice straw, pine wood, pig manure and sewage sludge. Chemosphere **218**, 624–631 (2019)
15. Rovira, P., Ramón Vallejo, V.: Labile, recalcitrant, and inert organic matter in Mediterranean forest soils. Soil Biol. Biochem. **39**, 202–215 (2017)
16. Chen, X., Yu, M., He, X., Zheng, M., Xi, B., Sun, Y., Fu, X., Su, J.: Fate of dissolved organic matter substructure in a full-scale wastewater treatment plant by using size exclusion chromatography multi-excitation-emission matrix analysis. J. Clean. Prod. **328**, 129677 (2021)
17. Stastny, K., Stepanova, H., Hlavova, K., Faldyna, M.: Identification and determination of deoxynivalenol (don) and deepoxy-deoxynivalenol (dom-1) in pig colostrum and serum using liquid chromatography in combination with high resolution mass spectrometry (LC-MS/MS (HR)). J. Chromatogr. B. **1126–1127**, 121735 (2019)
18. Bai, L., Zhao, Z., Wang, C., Wang, C., Liu, X., Jiang, H.: Multi-spectroscopic investigation on the complexation of tetracycline with dissolved organic matter derived from algae and macrophyte. Chemosphere **187**, 421–429 (2017)
19. Chen, B., Huang, W., Ma, S., Feng, M., Liu, C., Gu, X., Chen, K.: Characterization of chromophoric dissolved organic matter in the littoral zones of eutrophic lakes Taihu and Hongze during the algal bloom season. Water **10**, 861 (2018)
20. Qu, H.L., Guo, X.J., Chen, Y.S., Dai, B.L., He, J., Zhu, D.W.: Characterization of dissolved organic matter from effluents in a dry anaerobic digestion process using spectroscopic techniques and multivariate statistical analysis. Waste Biomass Valorization **8**, 793–802 (2017)
21. Guo, X.-J., He, X.-S., Li, C.-W., Li, N.-X.: The binding properties of copper and lead onto compost-derived DOM using Fourier-transform infrared, UV–vis and fluorescence spectra combined with two-dimensional correlation analysis. J. Hazard. Mater. **365**, 457–466 (2019)
22. Liu, X., Renard, C., Bureau, S., Bourvellec, C.L.: Revisiting the contribution of ATR-FTIR spectroscopy to characterize plant cell wall polysaccharides. Carbohydr. Polym. **263**, 117935 (2021)
23. Dhote, S., Dixit, S.: Water quality improvement through macrophytes—a review. Environ. Monit. Assess. **152**, 149–153 (2009)
24. He, Y., Song, N., Jiang, H.L.: Effects of dissolved organic matter leaching from macrophyte litter on black water events in shallow lakes. Environ. Sci. Pollut. Res. **25**, 9928–9939 (2018)

25. Welsch, M., Yavitt, J.B.: Early stages of decay of *Lythrum salicaria* L. and *Typha latifolia* L. in a standing-dead position. Aquat. Bot. **75**, 45–57 (2003)
26. Al-Wabel, M.I., Al-Omran, A., El-Naggar, A.H., Nadeem, M., Usman, A.R.A.: Pyrolysis temperature induced changes in characteristics and chemical composition of biochar produced from Conocarpus wastes. Bioresour. Technol. **131**, 374–379 (2013)
27. ASTM: D1762–84 Standard Test Method for Chemical Analysis of Wood Charcoal. ASTM International, West Conshohocken (2007)
28. Ohno, T., He, Z.: Fluorescence spectroscopic analysis of organic matter fractions: the current status and a tutorial case study. In: He, Z. (ed.) Environmental Chemistry of Animal Manure, pp. 83–103. Nova Science Publishers, New York (2011)
29. Ni, M., Li, S.: Biodegradability of riverine dissolved organic carbon in a dry-hot valley region: initial trophic controls and variations in chemical composition. J. Hydrol. **574**, 430–435 (2019)
30. Henderson, R.K., Andy, B., Parsons, S.A., Jefferson, B.: Characterisation of algogenic organic matter extracted from cyanobacteria, green algae and diatoms. Water Res. **42**, 3435–3445 (2008)
31. Huguet, A., Vacher, L., Relexans, S., Saubusse, S., Froidefond, J.M., Parlanti, E.: Properties of fluorescent dissolved organic matter in the Gironde estuary. Org. Geochem. **40**, 706–719 (2009)
32. Zsolnay, A., Baigar, E., Jimenez, M., Steinweg, B., Saccomandi, F.: Differentiating with fluorescence spectroscopy the sources of dissolved organic matter in soils subjected to drying. Chemosphere **38**, 45–50 (1999)
33. Hur, J., Park, M.-H., Schlautman, M.A.: Microbial transformation of dissolved leaf litter organic matter and its effects on selected organic matter operational descriptors. Environ. Sci. Technol. **43**, 2315–2321 (2009)
34. Murphy, K.R., Stedmon, C.A., Graeber, D., Bro, R.: Fluorescence spectroscopy and multi-way techniques. Parafac. Anal. Methods **5**, 6557–6566 (2013)
35. Noda, I., Ozaki, Y.: Two-Dimensional Correlation Spectroscopy: Applications in Vibrational and Optical Spectroscopy. Wiley, Chichester (2005)
36. He, Z., Mao, J., Honeycutt, C.W., Ohno, T., Hunt, J.F., Cade-Menun, B.J.: Characterization of plant-derived water extractable organic matter by multiple spectroscopic techniques. Biol. Fertil. Soils **45**, 609–616 (2009)
37. Xu, J., Wang, Y., Gao, D., Yan, Z., Gao, C., Wang, L.: Optical properties and spatial distribution of chromophoric dissolved organic matter (CDOM) in Poyang lake, China. J. Great Lakes Res. **43**, 700–709 (2017)
38. Liu, C.H., Chu, W., Li, H., Boyd, S.A., Teppen, B.J., Mao, J., Lehmann, J., Zhang, W.: Quantification and characterization of dissolved organic carbon from biochars. Geoderma **335**, 161–169 (2019)
39. Lin, C.W., Wu, C.-H., Tang, C.T., Chang, S.H.: Novel oxygen-releasing immobilized cell beads for bioremediation of BTEX-contaminated water. Bioresour. Technol. **124**, 45–51 (2012)
40. Martias, C., Tedetti, M., Lantoine, F., Jamet, L., Dupouy, C.: Characterization and sources of colored dissolved organic matter in a coral reef ecosystem subject to ultramafic erosion pressure (New Caledonia, southwest Pacific). Sci. Total Environ. **616**, 438–452 (2018)
41. Matilainen, A., Gjessing, E.T., Lahtinen, T., Hed, L., Bhatnagar, A., Sillanpää, M.: An overview of the methods used in the characterisation of natural organic matter (NOM) in relation to drinking water treatment. Chemosphere **83**, 1431–1442 (2011)
42. Burhenne, L., Messmer, J., Aicher, T., Laborie, M.-P.: The effect of the biomass components lignin, cellulose and hemicellulose on TGA and fixed bed pyrolysis. J. Anal. Appl. Pyrolysis **101**, 177–184 (2013)
43. Murphy, K.R., Bro, R., Stedmon, C.A.: Chemometric analysis of organic matter fluorescence. In: Coble, P.G., Lead, J., Baker, A., Reynolds, D.M., Spencer, R.G.M. (eds.) Aquatic Organic Matter Fluorescence, pp. 339–375. Cambridge University Press, New York (2014)
44. Osburn, C.L., Handsel, L.T., Mikan, M.P., Paerl, H.W., Montgomery, M.T.: Fluorescence tracking of dissolved and particulate organic matter quality in a river-dominated estuary. Environ. Sci. Technol. **46**, 8628–8636 (2012)
45. Lambert, T., Bouillon, S., Darchambeau, F., Massicotte, P., Borges, A.V.: Shift in the chemical composition of dissolved organic matter in the Congo river network. Biogeosciences **13**, 5405–5420 (2016)
46. Søndergaard, M., Stedmon, C.A., Borch, N.H.: Fate of terrigenous dissolved organic matter (DOM) in estuaries: aggregation and bioavailability. Ophelia **57**, 161–176 (2003)
47. Wheeler, K., Levia, D., Hudson, J.: Tracking senescence-induced patterns in leaf litter leachate using parallel factor analysis (Parafac) modeling and self-organizing maps. J. Geophys. Res. Biogeosci. **122**, 2233–2250 (2017)
48. Podgorski, D.C., Zito, P., Mcguire, J.T., Martinovic-Weigelt, D., Cozzarelli, I.M., Bekins, B.A., Spencer, R.G.M.: Examining natural attenuation and acute toxicity of petroleum-derived dissolved organic matter with optical spectroscopy. Environ. Sci. Technol. **52**, 6157–6166 (2018)
49. Cawley, K.M., Ding, Y., Fourqurean, J., Jaffé, R.: Characterising the sources and fate of dissolved organic matter in shark bay, Australia: a preliminary study using optical properties and stable carbon isotopes. Mar. Freshw. Res. **63**, 1098–1107 (2012)
50. Kothawala, D.N., von Wachenfeldt, E., Koehler, B., Tranvik, L.J.: Selective loss and preservation of lake water dissolved organic matter fluorescence during long-term dark incubations. Sci. Total Environ. **433**, 238–246 (2012)
51. Graeber, D., Gelbrecht, J., Pusch, M.T., Anlanger, C., Schiller, D.V.: Agriculture has changed the amount and composition of dissolved organic matter in central European headwater streams. Sci. Total Environ. **438**, 435–446 (2012)
52. Li, P., Chen, L., Zhang, W., Huang, Q.: Spatiotemporal distribution, sources, and photobleaching imprint of dissolved organic matter in the Yangtze estuary and its adjacent sea using fluorescence and parallel factor analysis. PLoS ONE **10**, e0130852 (2015)
53. Liu, C., Du, Y., Yin, H., Fan, C., Chen, K., Zhong, J., Gu, X.: Exchanges of nitrogen and phosphorus across the sediment-water interface influenced by the external suspended particulate matter and the residual matter after dredging. Environ. Pollut. **246**, 207–216 (2019)
54. Osburn, C.L., Wigdahl, C.R., Fritz, S.C., Saros, J.E.: Dissolved organic matter composition and photoreactivity in prairie lakes of the U.S. great plains. Limnol. Oceanogr. **56**, 2371–2390 (2011)
55. Uchimiya, M., Liu, Z., Sistani, K.: Field-scale fluorescence fingerprinting of biochar-borne dissolved organic carbon. J. Environ. Manage. **169**, 184–190 (2016)
56. Li, M., Zhang, A., Wu, H., Liu, H., Lv, J.: Predicting potential release of dissolved organic matter from biochars derived from agricultural residues using fluorescence and ultraviolet absorbance. J. Hazard. Mater. **334**, 86–92 (2017)
57. Jiang, Y., Cao, W., Tian, X., Jia, T., Niu, G., Zhang, J., Yuan, L.: Adsorption behavior and affecting factor for naphthalene on sediment of the yellow river in Lanzhou section. Res. Environ. Sci. **31**, 1545–1553 (2018)
58. Awasthi, M.K., Wang, M., Chen, H., Wang, Q., Zhao, J., Ren, X., Li, D.-S., Awasthi, S.K., Shen, F., Li, R., et al.: Heterogeneity of biochar amendment to improve the carbon and nitrogen sequestration through reduce the greenhouse gases emissions during

sewage sludge composting. Bioresour. Technol. **224**, 428–438 (2017)
59. Hur, J., Lee, B.-M.: Characterization of binding site heterogeneity for copper within dissolved organic matter fractions using two-dimensional correlation fluorescence spectroscopy. Chemosphere **83**, 1603–1611 (2011)
60. Gui, X., Liu, C., Li, F., Wang, J.: Effect of pyrolysis temperature on the composition of dom in manure-derived biochar. Ecotoxicol. Environ. Saf. **197**, 110597 (2020)
61. Li, W., Zhang, F., Ye, Q., Wu, D., Wang, L., Yu, Y., Deng, B., Du, J.: Composition and copper binding properties of aquatic fulvic acids in eutrophic Taihu lake, China. Chemosphere **172**, 496–504 (2017)
62. Sandt, C., Waeytens, J., Deniset-Besseau, A., Nielsen-Leroux, C., Réjasse, A.: Use and misuse of FTIR spectroscopy for studying the bio-oxidation of plastics. Spectrochim. Acta Part A **258**, 119841 (2021)
63. Kovács, R., Csontos, M., Gyngysi, S., Elek, J., Erdélyi, Z.: Surface characterization of plasma-modified low density polyethylene by attenuated total reflectance Fourier-transform infrared (ATR-FTIR) spectroscopy combined with chemometrics. Polym. Test. **96**, 107080 (2021)
64. Liu, D., Lu, K., Yu, H., Gao, H., Xu, W.: Applying synchronous fluorescence spectroscopy conjunct second derivative and two-dimensional correlation to analyze the interactions of copper (II) with dissolved organic matter from an urbanized river. Talanta **235**, 122738 (2021)
65. Qian, L., Zhang, W., Yan, J., Han, L., Gao, W., Liu, R., Chen, M.: Effective removal of heavy metal by biochar colloids under different pyrolysis temperatures. Bioresour. Technol. **206**, 217–224 (2016)
66. Ciursă, P., Pauliuc, D., Dranca, F., Ropciuc, S., Oroian, M.: Detection of honey adulterated with agave, corn, inverted sugar, maple and rice syrups using FTIR analysis. Food Control **130**, 108266 (2021)
67. Huang, M., Li, Z., Luo, N.: Application potential of biochar in environment insight from degradation of biochar-derived DOM and complexation of DOM with heavy metals. Sci. Total Environ. **646**, 220–228 (2019)

Authors and Affiliations

Bingfa Chen[1] · Kaining Chen[2] · Shiqun Han[1] · Cheng Liu[2] · Muhua Feng[2] · Wei Huang[2] · Hui Cai[3]

✉ Kaining Chen
knchen@niglas.ac.cn

✉ Shiqun Han
shqunh@126.com

[1] Institute of Agricultural Resources and Environmental Sciences, Jiangsu Academy of Agricultural Sciences, Nanjing 210014, China

[2] State Key Laboratory of Lake Science and Environment, Nanjing Institute of Geography and Limnology, Chinese Academy of Sciences, Nanjing 210008, China

[3] Suzhou Yifante Environmental Remediation Co., Ltd, Suzhou 215010, China